XLVI CILAMCE
VITÓRIA - ES - BRAZIL - 2025
XLVI IBERO-LATIN AMERICAN CONGRESS ON COMPUTATIONAL METHODS IN ENGENEERING

Free vibration analysis of rods by the enhanced C^k-generalized finite element method

Diego Amadeu F. Torres

[1]*Dept. of Mechanical Engineering, Federal University of Technology of Paraná*
Avenida João Miguel Caram 731 Jardim Pioneiros, 86036-370, Paraná, Brazil
diego.amadeu@gmail.com

Abstract. Mesh-based smooth approximations endowed with the first degree of consistency can be built through the C^k-Generalized Finite Element Method (C^k-GFEM). This is accomplished by incorporating the Moving Least Squares (MLS) method in its procedure when computing the Partition of Unity (PoU) functions. Despite the widened PoU's supports demanded, the enhanced polynomial reproducibility yields solutions with a cost, in terms of degrees of freedom (dof), similar to those approximations provided by the original version of GFEM, with C^0 continuity, for a certain polynomial degree of the ansatz. Additionally, in the case of static loading, such modified PoU functions allow some advantages when using special enrichment functions for localized features, leading to an increase in the conditioning of the stiffness matrices comparable to the original GFEM (Torres, 2024). The present work discusses some results for the free vibration analysis of linear elastic straight rods, considering different levels of k-continuity and polynomial degrees, with both attributes uniformly applied along the domain. It is emphasized that the k-order of continuity can be adjusted separately from the polynomial degree. The findings indicate that a certain level of smoothness allows a better use of the dof in the sense that a greater number of discrete natural frequencies have physical meaning. This is in contrast to conventional finite element approximations with C^0-regularity, for which higher-order discrete modes deviate significantly from continuous ones.

Keywords: smooth approximations, enhanced consistency, C^k-GFEM, k-p-refinements, enrichment

1 Introduction

The C^k-GFEM [1] differs from its original version [2] in that it considers smooth PoU functions. The process of constructing the PoU functions begins with the implicit representation[1] of the boundary of the nodal clouds by means of boundary[2] functions, which vanish precisely there and grow toward the interior of the cloud. Such boundary functions are chosen with the desired smoothness and are the primarily responsible for the approximation continuity level. The set of boundary functions that define the perimeter of a cloud is then used to generate a nodal weighting function through its product. Finally, from the set of nodal weighting functions, the PoU functions are computed. Originally, this task was performed using the *Shepard*'s equation and, therefore, ended up limiting the polynomial reproducibility[3] of the set of PoU functions.

The latter, therefore, inherits the minimum smoothness exhibited by the boundary functions. Rational smooth PoU functions, such as the *Shepard* ones, will have more oscillating derivatives the smaller their supports are, and this feature may be attractive for higher-order vibration modes. The smoothness adjustment process can be done independently of the polynomial degree which will be applied via extrinsic enrichment, i.e., allowing completely decoupled p and k[4] refinements.

Since the zeroth order of consistency of the C^k-GFEM PoU functions is harmful, an improvement has been to include the first-degree polynomial intrinsically [5, 6]. The static rod deformation problem was studied in [5] and [6] considering, respectively, only polynomial enrichments and special enrichment functions in addition to polynomials. In the last, it has been shown that the first degree of consistency leads to less sensitivity with respect

[1]Implicit representation of a subset, by means of primitive objects, in the sense of the Constructive Solid Geometry [3].
[2]In the context of higher dimensions, it has been usual to refer to those as cloud edge functions [4].
[3]Shepard's PoU's render only zeroth-degree consistency, that is, approximations with no first-degree extrinsic enrichment cannot provide a constant strain field.
[4]Different orders of smoothness may be produced simply by choosing different boundary functions along the domain.

to the size of the enrichment zone while requiring the same computational cost, in terms of dof, as conventional C^0-GFEM and with a similar impact on conditioning.

In the analysis of free vibrations by numerical methods, the quality of the obtained spectrum is an important issue because the discrete modes generally deviate from the continuous ones as the order of the modes increases. Therefore, the present study seeks to investigate the performance of the enhanced C^k-GFEM in the computation of natural frequencies for straight elastic rods with constant cross-section area and Young's modulus.

The paper is organized as follows. In the following section, the discretized formulation of the model problem is presented. In Section 3, the methodology is established, and the criteria for ensuring the quality of the numerical integration are detailed, as well as the parameters used in the method to solve the generalized eigenvalue problem. The results are discussed in Section 4, and finally some conclusions are drawn.

2 Model problem

The variables and procedures involved in the following discussion are stated as usual, according to classical texts on the topic [7, 8]. Consider an elastic bar of length l, [m], such that $\Omega \equiv [0, l]$, with constant cross-sectional area A, [m^2], Young's Modulus E, [N/m^2], and mass density ρ, [kg/m^3]. Assume that the cross sections originally plane remain plane during deformation and that the only non-negligible displacement component is that parallel to the bar's longitudinal axis, denoted as $u(x,t)$, [m]. Using the linear constitutive relation $\sigma(x,t) = E\varepsilon(x,t)$, and the infinitesimal strain-displacement relationship $\varepsilon(x,t) = \partial/\partial x\ (u(x,t))$, the strong-form undamped equilibrium equation, for an external force per unit length $f(x,t)$, [N/m], is expressed in the following form:

$$\rho A \frac{\partial^2}{\partial t^2} u(x,t) = EA \frac{\partial^2}{\partial x^2} u(x,t) + f(x,t)\ , \quad \text{on } \Omega \times]0, T[\ , \tag{1}$$

for an open time interval of length $T > 0$.

The boundary / initial conditions, respectively, are stated as:

$$u = \bar{u} \ \text{ on } \ \Gamma_D \times]0, T[\ , \quad EA\frac{du}{dx} = \bar{f} \ \text{ on } \ \Gamma_N \times]0, T[\ , \quad u(x,0) = u_0(x) \ \text{ and } \ \frac{\partial}{\partial t} u(x,0) = \dot{u}_0(x) \ \ \forall x \in \Omega\ . \tag{2}$$

For the problems solved here, for simplicity and without loss of generality, homogeneous *Dirichlet* and *Neumann* boundary conditions are considered in such a way that:

$$u(0) = \bar{u} = 0 \quad \text{(fixed)} \quad , \quad -EA\frac{d}{dx} u(l) = \bar{f} = 0 \quad \text{(free)}\ , \tag{3}$$

for the Dirichlet and Neumann boundaries, respectively Γ_D and Γ_N.

The strong-form governing equation for the frequencies and mode shapes, which may be obtained by the method of separation of variables and considering null $f(x,t)$, is expressed as follows:

$$\lambda A \rho u(x) + EA \frac{d^2}{dx^2} u(x) = 0\ , \ \ \forall\ x \in \Omega\ . \tag{4}$$

The (continuous) non-trivial solutions of (4) are countably infinite. In (4), $\lambda = \omega^2$ is the space-time coupling parameter, with ω being the natural frequency. The corresponding weak formulation is given by the following expression:

$$EA \int_\Omega \frac{du(x)}{dx} \frac{dv(x)}{dx}\, dx - E\Big(v(x) A \frac{du(x)}{dx}\Big)\Big|_0^l - \lambda A \rho \int_\Omega u(x)\, v(x)\, dx = 0\ , \tag{5}$$

for admissible test functions $v(x) \in \mathcal{H}^1(\Omega)$, the *Hilbert* space of functions that, together with their derivatives up to first order, are square integrable in the *Lebesgue* sense. The second term in 5 vanishes because $v(0) = 0$ on Γ_D, whereas on Γ_N, $d/dx\,(u(l)) = 0$. Consequently, the generalized eigenvalue problem may be stated as: to find a pair (λ, u), with $u \in \mathcal{H}^1(\Omega)$, satisfying the boundary conditions, and $\lambda \in \mathbb{R}$ such that:

$$\mathcal{B}\big(u(x), v(x)\big) - \lambda\big(u(x), \rho v(x)\big) = 0\ , \tag{6}$$

where

$$\mathcal{B}\big(u(x), v(x)\big) \equiv EA \int_0^l \frac{du}{dx} \frac{dv}{dx}\, dx \quad \text{and} \quad \big(u(x), \rho v(x)\big) \equiv A\rho \int_0^l u\, v\, dx\ . \tag{7}$$

The discretized weakened equilibrium problem is formulated in its irreducible version [8, 9]. Then, for a system with a finite number of dof, an approximation for the field $u(x,t)$, considering again the separation of variables, can be stated as:

$$u(x,t) = \phi_n(x)\, e^{i\,\omega_n\,t}\,, \tag{8}$$

where ω_n is the n-th natural frequency, and $\boldsymbol{\phi}_n$ is the n-th normal mode shape, whose spatial approximation is defined as $\phi_n(x) = \mathbf{N}(x)\,\mathbf{U}$, where $\mathbf{N}(x)$ is an array that contains the spatial approximation functions, and $\mathbf{U}$ is the vector of nodal parameters.

The discretized generalized eigenvalue problem that aims to find the eigenvalue λ_n and the associated eigenvector $\boldsymbol{\phi}_n \neq \mathbf{0}$ is:

$$\big(\mathbf{K} - \lambda_n \mathbf{M}\big)\boldsymbol{\phi}_n = \mathbf{0}\ . \tag{9}$$

The eigenvalue $\lambda_n = \omega_n^2$, with ω_n being the n-th natural frequency. The eigen functions $\boldsymbol{\phi}_n$ are determined only up to a multiplicative constant. In (9), $\mathbf{K}$ and $\mathbf{M}$ are the stiffness and the mass matrices, respectively, by assembling the elemental contributions. Herein, the consistent mass matrix is considered to avoid the underestimation effects of the lumped mass matrix. The elemental mass and stiffness matrices are defined respectively as:

$$\mathbf{M}^e = \rho A \int_{\Omega_e} \mathbf{N}^{e^T}\mathbf{N}^e\, d\Omega_e \quad \text{and} \quad \mathbf{K}^e = EA \int_{\Omega_e} \mathbf{B}^{e^T}\mathbf{B}^e\, d\Omega_e\,, \tag{10}$$

where $\mathbf{N}^e$ is the array that contains the approximation functions, and $\mathbf{B}^e$ is the array of spatial derivatives of the approximation functions within the element, for which the explicit dependence on x was omitted to simplify the notation.

3 Methodology

For the conventional C^k-GFEM, a cloud involves the two elements around its node, whereas widened clouds are required for the approach with enhanced consistency. In this work, a widened nodal cloud considers the two elements to the left and right of a given node to guarantee the realization of the MLS with degree one when computing the PoU functions. For internal nodes adjacent to those at the boundary, a ghost element outside the domain is created so as to have two elements on the left and right. In this case, both boundary functions will be required, even if one of the cloud boundary nodes is fictitious.

The procedure for constructing the nodal *weighting functions* can be briefly described as follows. Firstly, for each inner node in the discretization it is necessary to build two *boundary functions*, associated with the left and right boundaries of the corresponding *cloud*. For one node at the domain boundary, only its internal boundary function is needed. Such boundary functions need to have as many zero derivatives at their corresponding cloud ends to ensure the smoothness intended. Secondly, it is necessary to compute the product between the boundary functions of each cloud, whose result is the weighting function itself.

For the smooth approximations herein, a uniform k-refinement is obtained by considering boundary functions with progressively increasing continuities, such that $k = 1, 2, 3$ can be achieved using polynomial boundary functions with polynomial degree $p = 2, 3, 4$, respectively (see [4]). On the other hand, the maximum continuity, $k = \infty$, is obtained by applying exponential boundary functions [1]. Consequently, the weighting functions inherit the continuity of the boundary functions.

Finally, the weighting functions are used to compute the PoU functions. The PoU functions are MLS functions, having degree zero (Shepard equation) for C^k-GFEM [1], and degree one for its version with enhanced consistency/reproducibility, as described in [5]. In the following, this enhanced version will be referred to as the MLS-PoU-based approach.

For the present study, only uniform polynomial extrinsic enrichment was applied considering a set of four uniform nested meshes, with $5, 10$, 20 and 40 elements, denoted as M5, M10, M20, and M40, respectively, to guarantee the inclusion property[5].

Except for C^0-GFEM when only polynomial enrichments are used, the required number of integration points cannot be estimated since the basis functions are not essentially polynomial[6]. Thus, the numerical integration quality for both elemental stiffness and mass matrices, $\mathbf{K}_e$ and $\mathbf{M}_e$, respectively, was ensured by using progressively growing Gauss-Legendre quadrature rules, in each element, until the relative deviation between the entities obtained with the $s-1$ and s-th quadratures reached a pre-established tolerance, using:

[5] If the associated functions subspace of a given mesh is contained in the associated functions subspace of the next one, them the error decreases from mesh to mesh monotonically as $h \to 0$ [9].

[6] The PoU functions for the smooth GFEM versions can be considered as rational functions.

$$\|\mathbf{K}_e\| = \sqrt{\sum_{i=1}^{\text{dof}_e}\sum_{j=1}^{\text{dof}_e} k_{ij}^2} \quad , \quad \|\mathbf{M}_e\| = \sqrt{\sum_{i=1}^{\text{dof}_e}\sum_{j=1}^{\text{dof}_e} m_{ij}^2} \quad \text{, and} \quad \text{rel. dev.} = \frac{\left(\|\bullet\|^s - \|\bullet\|^{s-1}\right)}{\|\bullet\|^{s-1}} \,, \tag{11}$$

where dof_e is the number of dof for a given element.

The tolerance was specified as 10^{-11} for both $\mathbf{K}_e$ and $\mathbf{M}_e$, for the MLS-PoU-based GFEM, while 10^{-12} was chosen for the C^0- and C^k-GFEMs. MLS-PoU-based approximations can demand a less restrictive tolerance because their computation involves many more operations in addition to the solution of a point-wise system of equations, which can cause fluctuations[7] in the rel. dev. (11) at levels of the order of 10^{-11} or lower.

The generalized eigenvalue problem (9) was solved with the rank-completing perturbation method [10], using the `singgep` subroutine[8] with $\tau = 10^{-2}$, seeking to extract all possible eigenvalues, to obtain the full spectrum, as well as the convergence rates for the first three natural frequencies, in the case of h-refinement.

Some preliminary tests were performed to compare the effects of different continuity orders, mainly. For the problem of longitudinal structural vibration of an elastic rod, considering the boundary conditions (3), the exact values of the natural frequencies [7] can be computed as:

$$\omega_n = \frac{(2n-1)\pi}{2l}\left(\frac{E}{\rho}\right)^{1/2} \,, \; n = 1, 2, 3, \cdots \,. \tag{12}$$

For the calculations performed, EA and ρ were considered as 1.0 N and 1.0 kg/m^3, respectively, and the length l was 3.0 m.

Firstly, the results for the h version, using fixed degree $b = 1$, for the first three natural frequencies, will be shown to verify the impact of the parameter k on the order of convergence. Furthermore, still focusing on particular natural frequencies, the convergence rates for the fundamental frequency will be shown for degrees $b = 1$ and $b = 2$, and for the second and third natural frequencies for the degree $b = 1$. In the sequence, all spectra will be displayed considering polynomial degrees up to $b = 3$ and the mesh M20, using different orders of smoothness.

4 Results and discussion

It should be remarked that the polynomial degree spanned by the basis functions depends both on the degree of the PoU itself and on the extrinsically applied polynomial enrichment. In previous studies [12–14], it has been customary to consider b as the resulting degree of a numerical approximation. Thus, for the C^0-GFEM as well as for the MLS-PoU-based approach, $b = p + 1$, with p being the degree of extrinsic polynomial enrichment. Then, for a given degree b, the C^k-GFEM requires more extrinsic polynomial enrichment, consequently generating more dof, since its PoU has only degree zero. Then, the PoU functions for the C^0-GFEM as well as for the MLS-based C^k-GFEM can exactly represent the rigid body motion and the constant strain state, which is an advantage compared to the original version of the C^k-GFEM.

4.1 *h*-Convergence rates for the first three frequencies

Figure 1 shows the approximation behavior facing the h-refinement, considering different continuities, for the first three natural frequencies. Figures 1(a) and (b) show the h-convergence for the first natural frequency, whereas figures 1(c) and (d) are associated with the second natural frequency, and figures 1(e) and (f) are for the third one.

The relative error on the vertical axes is similar to that considered in [15]. Note that n_{el}, for the horizontal axis, is the number of elements. It was decided to separate the results for MLS-PoU-based GFEM and C^k-GFEM as the orders of magnitude are very different.

As a reference, the results for the C^0-GFEM solutions[9] are displayed in all graphics, and it is possible to confirm that the order of convergence for the frequencies is $O(h^{2b})$ [15], for the solution with the lowest regularity.

Remarkably, the error level for all smooth approximations is lower than that observed for the C^0 approximations. For the C^k-GFEM approximations, as the natural frequency order increases, it becomes more evident that the error evolution has not yet reached an asymptotic behavior, indicating that meshes with more than 20 elements are necessary to truly obtain a convergence rate. However, it is already possible to expect that the convergence rates for all C^k-GFEM solutions tend to reach the values obtained for C^0-GFEM.

[7] Of course, an adjustment of such a tolerance needs to be made before running the numerical experiments.

[8] Available in [11]. Criteria for infinite eigenvalues: infgap $= 0.95$ and fingap $= 0.01$.

[9] For $b = 1$, such case is equal to the linear FEM, that is based on tent functions.

Furthermore, it can be seen that as the order of the natural frequency increases, the convergence rates of the MLS-PoU-based solutions always exceed those exhibited by the C^0 counterpart.

Typically, higher-degree basis functions lead to higher accuracy as the mesh is refined [15]. Then, the convergence rates for the fundamental frequency, considering degrees up to $b = 2$ uniformly applied along the domain, are shown in Table 1 along with the coefficient of determination R^2 for a linear approximation, considering the four points even if the asymptotic range has not been achieved for some of the C^k-GFEM cases. Noticeably, for the MLS-PoU-based GFEM solutions with $b = 1$, higher convergence rates are obtained for all smoothness, except for the C^1 case. Furthermore, higher convergence rates occur for the C^3 solution with $b = 2$, for both C^k-GFEM and MLS-PoU-based GFEM.

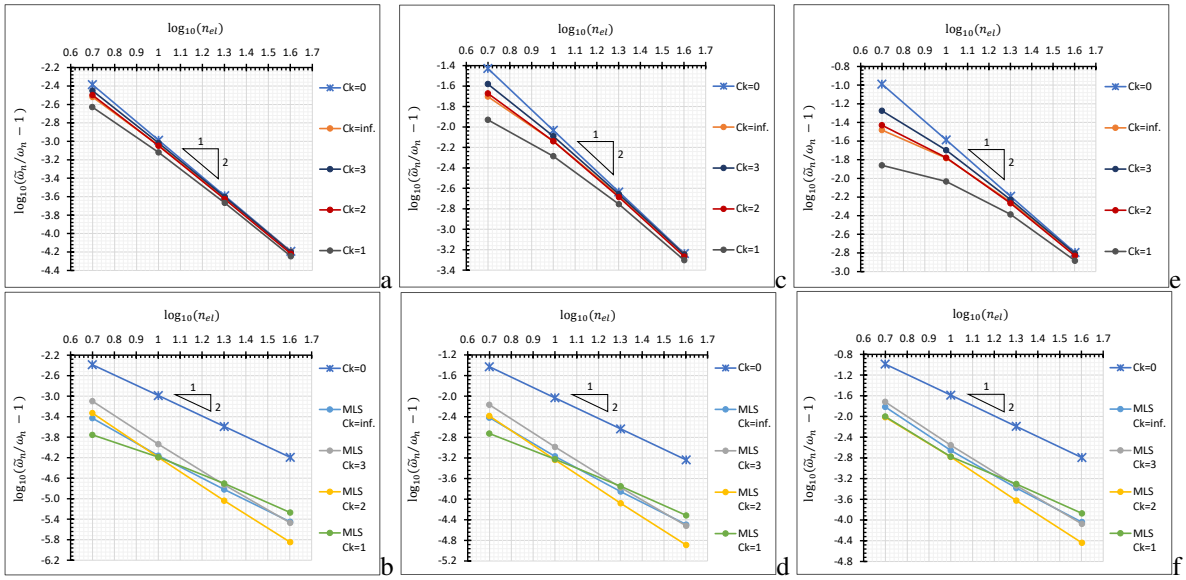


Figure 1. Order of convergence for the first three natural frequencies considering approximations with $b = 1$ and different k-continuities. (a) and (b) for the first frequency. (c) and (d) for the second frequency. (e) and (f) for the third frequency.

Table 2 shows the convergence rates for the second and third natural frequencies when the approximation degree is $b = 1$. Once again, smooth GFEM approximations with enhanced consistency exhibit significantly improved convergence rates compared to those exhibited by C^0-GFEM, evidencing a positive impact of smoothness on the computation of natural frequencies.

Table 1. Convergence rates for the first natural frequency, for different continuities, considering approximations with polynomial degree $b = 1$ and 2.

degree		C^0	C^∞	C^3	C^2	C^1	MLS C^∞	MLS C^3	MLS C^2	MLS C^1
$b = 1$	rate	−2.00	−1.86	−1.94	−1.91	−1.73	−2.23	−2.63	−2.79	−1.68
	R^2	1.0	1.0	1.0	1.0	1.0	1.0	1.0	1.0	1.0
$b = 2$	rate	−4.00	−3.95	−4.34	−3.79	−3.92	−3.60	−4.48	−3.74	−4.05
	R^2	1.0	1.0	1.0	1.0	1.0	1.0	1.0	1.0	1.0

Table 2. Convergence rates for the second and third natural frequencies, for different continuities, considering approximations with polynomial degree $b = 1$.

freq. order		C^0	C^∞	C^3	C^2	C^1	MLS C^∞	MLS C^3	MLS C^2	MLS C^1
$n = 2$	rate	−2.00	−1.71	−1.85	−1.77	−1.52	−2.30	−2.60	−2.78	−1.76
	R^2	1.0	1.0	1.0	1.0	1.0	1.0	1.0	1.0	1.0
$n = 3$	rate	−2.00	−1.48	−1.70	−1.56	−1.14	−2.46	−2.61	−2.70	−2.04
	R^2	1.0	0.98	1.0	0.99	0.96	1.0	1.0	1.0	0.99

4.2 Influence of the continuity on the spectra

Discrete spectra obtained using different continuities, for polynomial degrees up to $b = 3$, are also discussed. Figure 2 shows the resulting natural frequencies, $\tilde{\omega}_n$, normalized with respect to the exact solution (12), and plotted versus the mode number, n, normalized by the total number of available discrete frequencies[10], N. For this purpose, the mesh with 20 elements, M20, was considered.

Once more, the results for the MLS-PoU-based GFEM are displayed apart from the results obtained with the C^k-GFEM, and for each degree b, the solutions from C^0-GFEM are shown jointly with both smooth versions of GFEM. Figures 2(a) and (b) are related to $b = 1$, figures 2(c) and (d) refer to $b = 2$, while figures 2(e) and (f) are for $b = 3$.

To produce the spectra, different values of N were considered, depending on the type of approximation. It should be noted that the spectra for the C^k-GFEM approximations show more points because they involve more dof than the other approximations for a given polynomial degree b, since their PoU functions have zeroth degree.

From Figure 2(a), it is possible to see that only about the first 25% of the discrete frequencies deviates around 2% or less from the exact values. Noticeably, about 75% of the first natural frequencies for the C^k-GFEM case with $k = 1$ have an error smaller than 2%. Still considering $b = 1$, for the MLS-PoU-based GFEM approximations (Figure 2(b)), the continuities $k = 2$ and $k = 3$ exhibit at least 80% of the first frequencies with errors smaller than 2%.

Figure 2(c) shows that C^0-GFEM with $b = 2$ behaves very similarly to quadratic FEM, as well as the spectrum for C^0-GFEM with $b = 3$, Figure 2(e), is very close to that obtained for cubic FEM [15]. For FEM, it is well known that an acoustical branch occurs for $n/N < 0.5$ and an optical branch for $n/N > 0.5$, for quadratic elements, whereas for cubic elements, the optical branch arises for $n/N > 0.67$. Typically, in finite element analysis, the frequencies associated with the optical branch are regarded spurious.

Regarding the C^k-GFEM approximations, for the first two degrees b, the continuity $k = 1$ provided better performance. However, for $b = 3$, the continuities $k = 2$ and $k = \infty$ provided a greater number (around 65%) of natural frequencies with errors less than 2%, see Figure 1(e).

When $b = 2$, the spectrum generated by the MLS-PoU-based version with $k = 1$ is very similar to that typical of the C^0 approximations, as shown in Figure 2(d), where it is also possible to see that about 70% of the first natural frequencies have an error smaller than 2%, in the case of $k = 3$. For $b = 3$, the MLS-PoU-based approximations with continuities $k = 2$ and $k = \infty$ virtually have the same number of frequencies with errors smaller than 2% compared to the version C^0, as seen in Figure 2(f). Only the case with $k = 3$ provides a slightly larger number of frequencies with relative errors below the mentioned level.

Finally, as also noted in [15] , the anomalous frequencies at the extreme of the spectrum increase as the degree b increases, and some dependence on the level of smoothness is also observed.

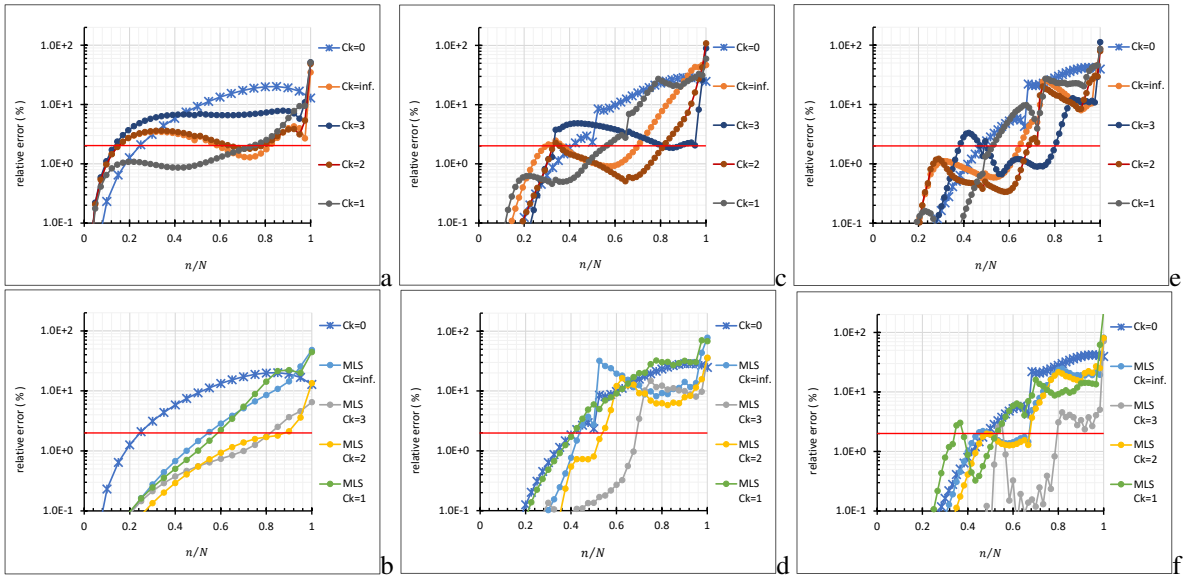


Figure 2. Normalized discrete spectra considering different k-continuities, for the mesh M20. (a) and (b) for approximations with $b = 1$. (c) and (d) for approximations with $b = 2$. (e) and (f) for approximations with $b = 3$.

[10]Taking into account any possible rank deficiency, due to linear dependence.

5 Conclusions

Some level of smoothness can positively impact the rate of convergence in the presence of h-refinement when computing natural frequencies, especially if the PoU functions has enhanced consistency.

On the other hand, considering the frequency spectra, for the lowest polynomial degree b, approximations based on smooth PoU functions with enhanced consistency show a significant advantage in obtaining physically meaningful discrete natural frequencies for all the levels of continuity assessed. Furthermore, the dependence on the smoothness of the approximation is evident to some extent, both for the original C^k-GFEM and for the version with enhanced consistency, as the polynomial degree b increases.

Authorship statement. The author hereby confirm that he is the sole liable person responsible for the authorship of this work, and that all material that has been herein included as part of the present paper is either the property (and authorship) of the author, or has the permission of the owners to be included here.

References

[1] C. A. Duarte, D. J. Kim, and D. M. Quaresma. Arbitrarily smooth generalized finite element method. *Computer Methods in Applied Mechanics and Engineering*, vol. 196, n. 1-3, pp. 33–56, 2006.

[2] C. A. Duarte, I. Babuška, and J. T. Oden. Generalized finite element methods for three-dimensional structural mechanics problems. *Computers and Structures*, vol. 77, n. 2, pp. 215–232, 2000.

[3] V. L. Shapiro, T. I. Sheiko, V. Shapiro, and I. Tsukanov. Transfinite interpolation over implicitly defined sets. *Computer Aided Geometry Design*, vol. 18, pp. 195–220, 2001.

[4] C. S. de Barcellos, P. T. R. Mendonça, and C. A. Duarte. A C^k continuous generalized finite element formulation applied to laminated Kirchhoff plate model. *Computational Mechanics*, vol. 44, pp. 377–393, 2009.

[5] M. Garbuio and D. A. F. Torres. Improving the polynomial reproducibility for the partition of unity in the C^k-generalized FEM. In E. P. Bandarra Filho, ed, *Proceedings of the twenty-fifth International Congress of Mechanical Engineering (XXV COBEM)*, Uberlândia. Brazilian Association of Engineering and Mechanical Sciences – ABCM, 2019.

[6] D. A. F. Torres. C^k-Generalized FEM with enhanced consistency: application to the static elastic rod deformation problem. In *Proceedings of the forty-fifth Ibero-Latin American Congress on Computational Methods in Engineering (XLV CILAMCE)*, Maceió. Brazilian Association of Computational Methods in Engineering - ABMEC, 2024.

[7] S. S. Rao. *Vibration of continuous systems*. John Wiley & Sons, New Jersey, 2007.

[8] T. J. R. Hughes. *The finite element method: linear static and dynamic finite element analysis*. Prentice Hall, New Jersey, 1987.

[9] I. Babuška, J. R. Whiteman, and T. Strouboulis. *Finite elements: an introduction to the method and error estimation*. Oxford, New York, 2011.

[10] M. E. Hochstanbach, C. Mehl, and B. Plestenjak. Solving singular generalized eigenvalue problems by a rank-completing perturbation. *SIAM Journal on Matrix Analysis and Applications*, vol. 40, pp. 1022–1046, 2019.

[11] B. Plestenjak. *MultiParEig: Toolbox for multiparameter and singular eigenvalue problems*. MATLAB Central File Exchange. https://www.mathworks.com/matlabcentral/fileexchange/47844-multipareig - version 2.8.0.0 (Accessed: 2025-07-22), 2024.

[12] D. A. F. Torres, C. S. de Barcellos, and P. T. R. Mendonça. Effects of the smoothness of partitions of unity on the quality of representation of singular enrichments for GFEM/XFEM stress approximations around brittle cracks. *Computer Methods in Applied Mechanics and Engineering*, vol. 283, pp. 243–279, 2015.

[13] D. A. F. Torres, C. S. de Barcellos, and P. T. R. Mendonça. Smooth Generalized/eXtended FEM approximations in the computation of configurational forces in linear elastic fracture mechanics. *International Journal of Fracture*, vol. 219, n. 2, pp. 185–210, 2019.

[14] D. A. F. Torres. On the topological enrichment for crack modeling via the Generalized/eXtended FEM: a novel discussion considering smooth partitions of unity. *Engineering Computations*, vol. 38, n. 9, pp. 3517–3547, 2021.

[15] J. A. Cottrell, A. Reali, Y. Bazilevs, and T. Hughes. Isogeometric analysis of structural vibrations. *Computer Methods in Applied Mechanics and Engineering*, vol. 195, pp. 5257–5296, 2006.